Send Orders for Reprints to reprints@benthamscience.ae

The Open Civil Engineering Journal, 2018, *12*, 1-20

The Open Civil Engineering Journal

Content list available at: www.benthamopen.com/TOCIEJ/

DOI: 10.2174/1874149501812010001

RESEARCH ARTICLE

Design of SMA-Brace Devices for the Seismic Retrofit of Steel CBF

Ernesto Grande* and Giampietro Ruotolo

Department of Sustainability Engineering, University Guglielmo Marconi, via Plinio 44, 00193, Roma, Italy

Received: November 02, 2017 Revised: January 12, 2018 Accepted: January 17, 2018

Abstract:

Introduction:

Retrofit interventions are often performed by introducing in structures dissipative devices able to improve the global seismic response particularly in terms of energy dissipation capacity. In the case of Concentric Braced Steel Frames (CBF), these devices are generally introduced in the form of brace elements made of different materials and based on different dissipation mechanisms. Their design is strictly related to both the characteristics of the selected device and, also, to the own peculiarities of the structural system involved in the retrofit intervention.

Methods:

The paper presents a simple design approach for the seismic retrofit of non-ductile CBF through the use of Shape Memory Alloys (SMA) brace devices. The approach merges the potentialities of SMA materials and the main peculiarities of the truss-resistant mechanism of CBFs throughout a procedure based on a preliminary phase of assessment, an intermediate phase of requirements evaluation and a final phase of design of the retrofit intervention.

Results and Conclusion:

After a detailed explanation of the proposed approach, the results derived from non-linear time-history analyses developed with reference to three and five-story CBFs are presented in the paper.

Keywords: CBF, SMA, Retrofit, Non-linear time-history analyses, Brace devices.

1. INTRODUCTION

Innovative materials and retrofitting techniques play an important role in the field of seismic protection of structures. In particular, a wide variety of dissipative devices are now available on the market for both the design of new structures and the retrofit of the existing ones. The use of dissipative devices is mainly devoted to improve the energy dissipation capacity of structural systems while preserving the other structural members.

In the case of retrofit interventions, the choice of the type of dissipative device and the design of the retrofit intervention is dependent on many factors related to both the characteristics of the selected device and, also, to the own peculiarities of the involved structural system.

The present paper focuses on retrofit interventions for concentric braced steel frames (CBF) based on the use of SMA-brace devices. Indeed, CBF is a structural system configuration widely used for steel buildings thanks to the truss mechanism characterizing its behavior toward lateral forces, which provides high levels of lateral stiffness in comparison to other structural typologies. On the other hand, buckling phenomena involving members and connections generally lead to either fragile global failure mechanisms of CBFs or significant losses of the global ductility and energy dissipation [1 - 3]. This occurs in particular when an elastic design of CBFs is performed, as suggested by past

* Address correspondence to this author at the Department of Sustainability Engineering, University Guglielmo Marconi, *via* Plinio 44, 00193, Roma, Italy; Tel: +3906377251; E-mail: e.grande@unimarconi.it

codes. Consequently, retrofit interventions involving this structural typology are mainly devoted to improve the seismic response in terms of ductility and energy dissipation capacity [3].

In fact, in agreement with modern standard codes [4, 5] which recognize the role of the braces in guarantying a ductile and dissipative seismic behavior of CBFs, different retrofit strategies for CBFs are based on the use of 'dissipative' braces [6 - 17]. Among these, particular relevance assume the SMA-brace devices based on the use of shape memory alloys materials in the form of wires or bars [10 - 15]. Indeed, thanks to the dissipative and full-recentering peculiarities of SMA materials, these devices allow to provide seismic energy dissipations, while avoiding residual inelastic deformations of structures.

The studies available in the current literature mainly concern experimental and numerical characterization of both SMA materials and SMA-devices. On the other hand, differently from other types of dissipative braces, only few studies focus the attention on the seismic design of these systems particularly for the retrofit of existing structures [14 - 15]. Nevertheless, these studies mainly focus on showing the potentialities of SMA devices in improving the seismic response of structures. They generally present numerical analyses or experiments where it is underlined the ability of SMA-brace devices in improving the global energy dissipation capacity of structures. On the contrary, these studies do not devote particular attention to the development of approaches for the practical design of SMA-brace devices for the retrofit of existing structures, able to merge requirements/criticisms of structures and potentialities/features of SMA-brace devices.

In this context, the present paper aims at proposing a simple approach for the design of SMA-brace devices for the seismic retrofit of concentric braced steel frames characterized by a low-ductile seismic behavior, i.e. when the ultimate mechanism is governed by buckling phenomena involving the columns or the beams, or by failure phenomena of connections. In particular, starting from a design procedure recently proposed by the authors [17], the approach here proposed merges the peculiarities and the weaknesses generally characterizing the seismic behavior of non-ductile CBFs, with the strengths of the use of SMA-brace devices.

The procedure at the basis of the proposed design approach is presented in detail in the first part of the paper. Then, numerical non-linear time-history analyses devoted to assess the reliability of the proposed approach are reported in the second part of the paper. A conclusive section is finally provided.

2. MATERIALS AND METHODS

2.1. Proposed Approach

The proposed design approach is based on three main steps strictly connected among them.

The first step (*seismic assessment*) is devoted to identify the need to provide retrofit interventions by comparing the global seismic resistance of CBFs, derived by considering the potential failure mechanism, and the design seismic actions evaluated according to the national guidelines.

The second step (*damping requirement*) aims at evaluating the damping level required to the retrofitted solution for satisfying the seismic demand emerged from the previous step.

The third step (*retrofit solution*) aims at deriving the parameters of the SMA-brace devices inserted in the CBF in lieu of one or more steel diagonals for guaranteeing the required level of damping.

The whole procedure at the basis of the proposed approach considers simple formulas carried out by considering the truss mechanism of CBF structural systems [2, 3], and considering retrofit interventions simply based on the substitution of some steel diagonals through SMA-brace devices. Moreover, although the possible retrofit solutions could differ in terms of number and arrangement of the SMA-brace devices, the whole procedure is developed by considering a retrofit intervention devoted to assure that:

- all the SMA-brace devices are designed in order to exhibit an equivalent viscous damping ratio ($\xi_{hyst,\max,i}^{SMA}$) corresponding to the attainment of the stress $\sigma_{f,AS}^{SMA}$ of the SMA material at the end of the Austenite-Martensite transformation phase (Fig. **1**);
- the SMA-brace devices have to preserve all the steel diagonals of the CBF toward the yielding, and the column and beam members toward buckling phenomena.

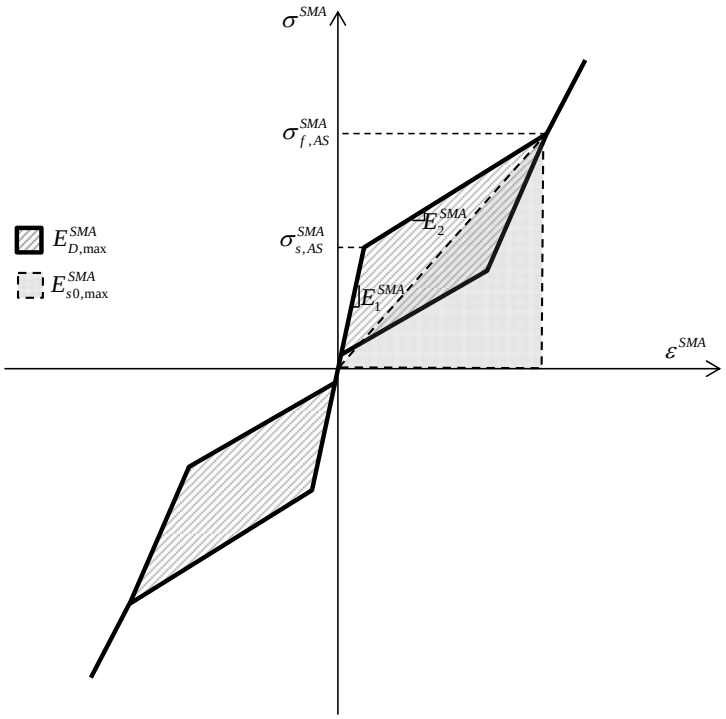

Fig. (1). Schematization of the constitutive law of the SMA material

These two design criteria are aimed at optimizing the amount of SMA material composing the devices by exploiting its hysteretic and recentering peculiarities, and, moreover, to ensure that the SMA-brace devices are the only dissipative members of CBF.

The parameters derived from the proposed approach in terms of amount of SMA material, concern the characteristics of SMA-braced devices composed of a rigid part and a deformable portion just made of SMA in the form of wires or bars. This assumption aims at reproducing the configuration and the behavior of the SMA-braced device proposed by Dolce *et al*., 2000 [13]. Indeed, it is simply composed of two concentric pipes that can move mutually, connected by SMA wires or bars behaving in tension for both tensile and compression forces arising in the brace.

2.2. Step 1 – Seismic Assessment

The first step concerns the seismic assessment of the CBF through a simple procedure devoted to: (i) recognize the potential failure mechanism of the CBF, (ii) evaluate the corresponding seismic force V_b^*(capacity), (iii) compare this force with the design seismic force (demand) V_b furnished by standard codes.

In particular, according to the approach proposed in [2], considering the truss mechanism of CBF, the design gravity loads and the design seismic actions it is possible to derive the forces in the members (beams, columns, and diagonals) by using simple equilibrium considerations.

Then, considering the yield and buckling strength of the members of the CBF, the failure mechanism and the corresponding seismic base shear capacity V^*_b can be evaluated. The allowable seismic base shear V^*_b just corresponds to the attainment of the buckling of the columns or beams, or to the yielding of diagonals with high slenderness ratio values, in the case of low-ductile CBFs.

Finally, comparing the allowable seismic base shear and the seismic design base shear (V_b) derived from national guidelines, the required level of reduction of the seismic forces in terms of damping factor (η^*) can be evaluated:

$$\eta^* = \frac{V_b^*}{V_b} \tag{1}$$

In case of need of retrofit it results: $\eta^*<1$.

2.3. Step 2 – Damping Requirement

Considering the level of reduction of seismic forces derived from the previous step, the equivalent viscous damping ratio required for retrofitting the CBF can be obtained [18]:

$$\xi^{CBF} = \frac{10}{(\eta^*)^2} - 5 \tag{2}$$

The equivalent viscous damping coefficient of the retrofitted CBF can be assumed as the sum of the initial damping coefficient (ξ_I^{CBF}) into elastic range, and the hysteretic part due to the non-linear behavior (ξ_{hyst}^{CBF}):

$$\xi_{eff}^{CBF} = \xi_I^{CBF} + \xi_{hyst}^{CBF} \tag{3}$$

where, according to [19]; (Fig. **1**), the part corresponding to the non-linear response of the CBF can be obtained by introducing the concept of dissipated energy (E_D^{CBF}) and the stored energy (E_{s0}^{CBF}):

$$\xi_{hyst}^{CBF} = \frac{1}{4\pi}\frac{E_D^{CBF}}{E_{s0}^{CBF}} \tag{4}$$

In particular, since the SMA devices are the only brace elements contributing to the hysteretic damping of the retrofitted CBF, whilst steel diagonals and the other members have to remain in the elastic field, the dissipated energy of the CBF can be assumed coincident with the energy dissipated by the SMA-brace devices: $E_D^{CBF} = \sum_i E_{D,i}^{SMA}$, where $E_{D,i}^{SMA}$ is the hysteretic energy dissipated by the SMA-brace device located at the generic i-th story of the retrofitted CBF.

Considering **eqn.4**, the hysteretic energy dissipated by the SMA brace device is:

$$E_{D,i}^{SMA} = 4\pi\xi_{hyst,\max,i}^{SMA} E_{s0,i}^{SMA} = 2\pi\xi_{hyst,\max,i}^{SMA} N_{u,i}^{SMA} \Delta L_{u,i}^{SMA} \tag{5}$$

where the stored energy has been evaluated by accounting for the axial force ($N_{u,i}^{SMA}$) and the axial deformation ($\Delta_{u,i}^{SMA}$), both corresponding to the attainment of the equivalent viscous damping level of the SMA-brace device $\xi_{hyst,max,i}^{SMA}$.

On the other hand, the stored energy of the CBF is here evaluated by only considering the stored energy of the SMA-brace devices and the stored energy of the steel diagonals [17]:

$$E_{s0}^{CBF} = \sum_i \frac{1}{2} N_{u,i}^{SMA} \Delta L_{u,i}^{SMA} + \sum_{j \neq i} \frac{1}{2} N_j^{diag} \Delta L_j^{diag} \tag{6}$$

where N_j^{diag} and ΔL_j^{diag} are respectively the axial force and the axial deformation of the steel diagonals of the retrofitted CBF evaluated by considering the allowable seismic base shear V_b*.

2.4. Step 3 – Retrofit Solution

Considering the scheme of the CBF shown in Fig. (**2**), where tension-only steel diagonals are considered according to [2] and some SMA-brace devices are introduced in lieu of steel diagonals, subjected to the horizontal seismic forces corresponding to the allowable base shear V_b*, the axial forces and the axial deformations of these members are:

$$N_{u,i}^{SMA} = \frac{V_{b,i}^* \gamma_{V,i}}{\cos\theta_i}; \quad \Delta L_{u,i}^{SMA} = \frac{N_{u,i}^{SMA}}{K_{\sec,i}^{SMA}} \tag{7a}$$

$$N_j^{diag} = \frac{V_{b,j}^* \gamma_{V,j}}{\cos\theta_j}; \quad \Delta L_j^{diag} = \frac{N_j^{diag}}{K_{el,j}^{diag}} \tag{7b}$$

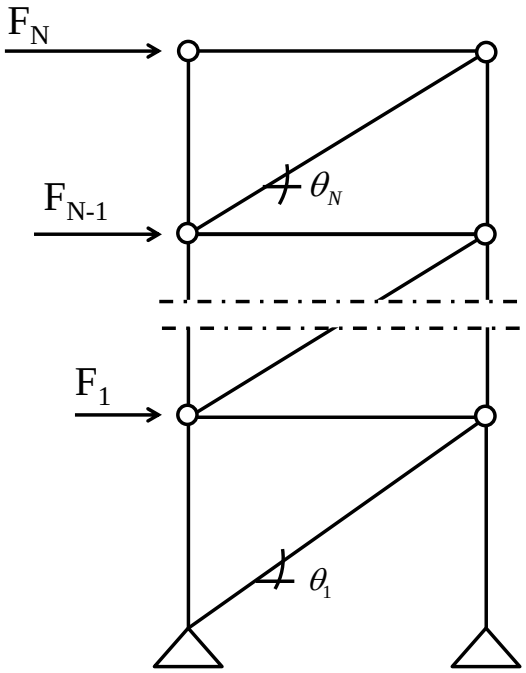

Fig. (2). Tension-only scheme of the CBF.

where $K_{sec,i}^{SMA}$ is the secant stiffness of the SMA brace device located at the story i (Fig. **3**), $K_{el,j}^{diag}$ is the elastic stiffness of the steel diagonal located at the story j and $\gamma_{V,i}$ is a factor depending on the distribution of the seismic story shear along the height of the CBF: it is equal to the ratio between the allowable shear $V_{b,i}^{*}$ at the story i of the CBF and the allowable base shear V_b*.

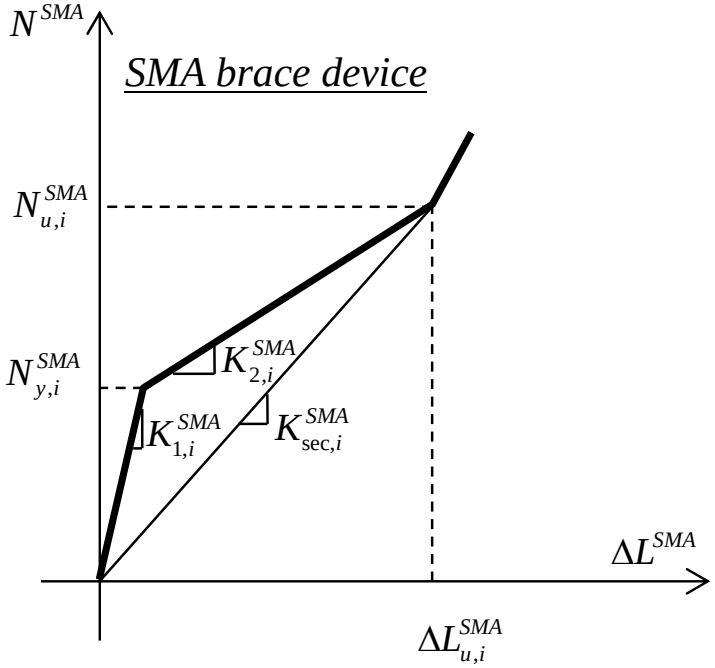

Fig. (3). Schematization of the axial behavior of the SMA brace device.

In particular, while $K_{sec,i}^{SMA}$ is an unknown of the procedure (it is indeed related to the characteristics of the SMA-brace device), $K_{el,j}^{diag}$ can be simply derived as:

$$K_{el,j}^{diag} = \frac{E_{steel} A_j^{diag}}{L_j^{diag}} \tag{8}$$

where E_{steel} is the Young's modulus of the steel material composing the diagonal and A_j^{diag}, L_j^{diag} are respectively the cross section area and the length of the steel diagonal located at the generic story j.

Taking into account **eqns.7**, the viscous damping ratio of the retrofitted CBF assumes the following form:

$$\xi_{eff}^{CBF} = \xi_I^{CBF} + \frac{\sum_i \frac{\xi_{hyst,\max,i}^{SMA} \gamma_{V,i}^2}{\cos^2\theta_i K_{\sec,i}^{SMA}}}{\sum_k \frac{\gamma_{V,k}^2}{\cos^2\theta_k K_{\sec,k}^{SMA}} + \sum_{j\neq i} \frac{\gamma_{V,j}^2}{\cos^2\theta_j K_{el,j}^{diag}}} \tag{9}$$

where the index i and k refers to the stories where the SMA-devices have been provided, the index j refers to the stories where are present the steel diagonals. The damping $\xi_{hyst,\max,i}^{SMA}$ can be directly derived from the constitutive law of the SMA material considering the dissipative energy and the stored energy (Fig. **1**). In the numerical applications presented in the following a value of $\xi_{hyst,\max,i}^{SMA}$ equal to 0.1157 has been obtained on the basis of the characteristics of the SMA material.

Then, imposing $\xi_{eff}^{CBF} = \xi^{CBF}$ and assuming a fixed number and arrangement of the SMA-brace devices in the CBF, the only unknowns of **eqn.9** are the values of the secant stiffness of the SMA-brace devices: an equation with one or more unknowns depending on the number of SMA-brace devices placed into the CBF.

Nevertheless, selecting a criterion for distributing the secant stiffness of the SMA-brace devices along the height of the CBF, **eqn.9** allows to derive the secant stiffness of each SMA-brace device composing the retrofitted solution.

Once the secant stiffness of SMA-brace devices has been derived, it is then possible to evaluate:

- the cross section area of the SMA-brace devices:

$$A_i^{SMA} = \frac{V_b^* \gamma_{V,i}}{\sigma_{f,AS}^{SMA} \cos\theta_i} \tag{10}$$

- their yielding and ultimate axial resistance:

$$N_{y,i}^{SMA} = \sigma_{s,AS}^{SMA} A_i^{SMA} \tag{11a}$$

$$N_{u,i}^{SMA} = \sigma_{f,AS}^{SMA} A_i^{SMA} \tag{11b}$$

- the elastic stiffness of the SMA-brace devices in the austenite phase:

$$K_{1,i}^{SMA} = \left(N_{y,i}^{SMA} + \frac{N_{u,i}^{SMA} - N_{y,i}^{SMA}}{\beta} \right) \frac{1}{\Delta L_{u,i}^{SMA}} \tag{12}$$

where $\beta = \frac{E_1^{SMA}}{E_2^{SMA}}$ . .

- the length of the deformable portion of the SMA-brace devices, corresponding to the length of wires or bars composing the device:

$$L_i^{SMA} = \frac{E_1^{SMA} A_i^{SMA}}{K_{1,i}^{SMA}} \quad \textbf{(13)}$$

3. CASE STUDIES AND RESULTS

The numerical applications reported in the paper are mainly devoted to assess the effectiveness of the proposed approach. For this aim, simple case studies consisting of three-story and five-story steel braced frames (Fig. **4a**, Table **1**; Fig. **5**, Table **2**) have been selected: they are denoted in the following CBF-3s and CBF-5s, respectively. Both the accounted cases are characterized by a non-ductile seismic behavior where the base columns represent the weak structural components: the allowable seismic base shear corresponds to the attainment of the buckling resistance of the base columns of the CBF. Then, in this case the goal of the retrofit intervention is to increase the energy dissipation capacity through the hysteretic behavior of SMA-braces, protecting the columns and beams toward buckling phenomena and the remaining steel diagonals of CBF toward the yielding.

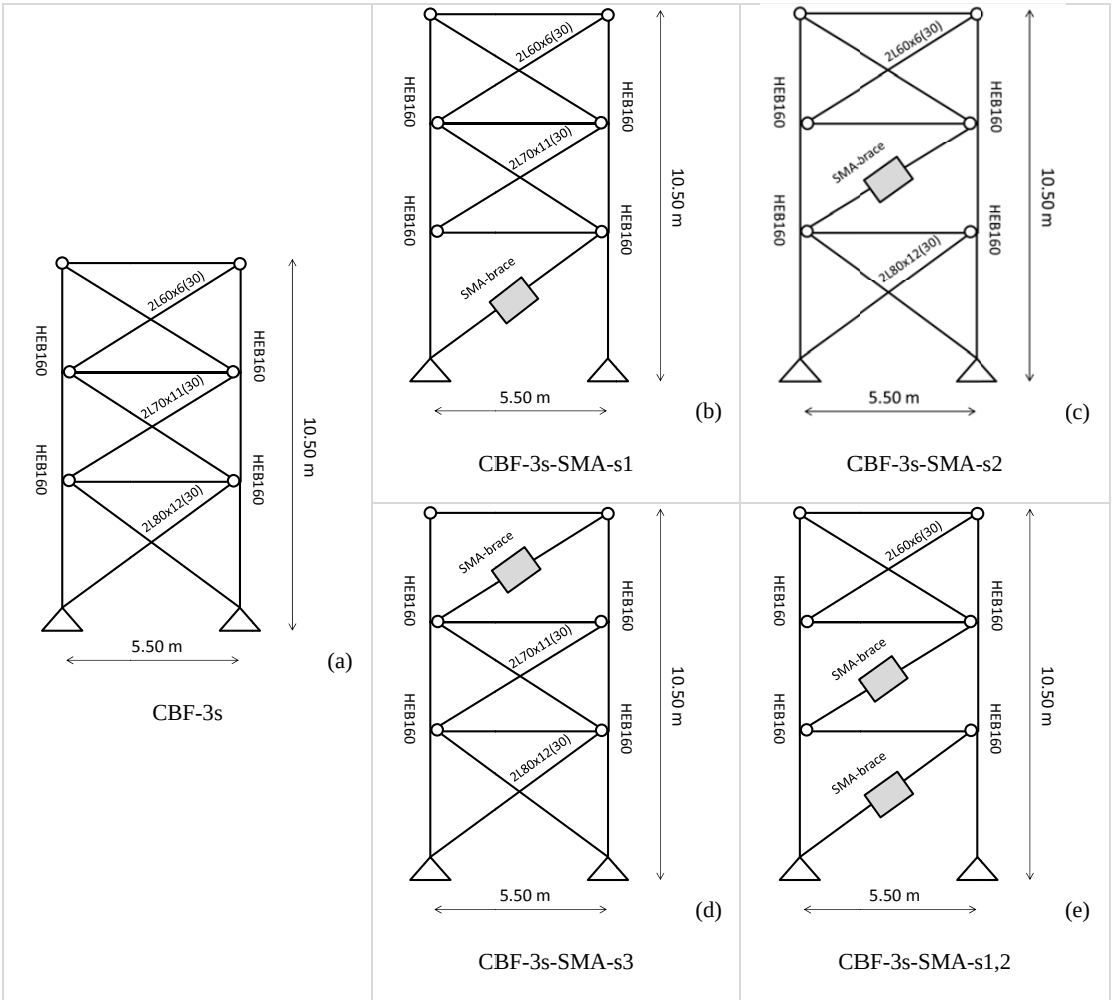

Fig. (4). Accounted three-story CBF cases.

Table 1. Parameters characterizing the un-retrofitted case of study: CBF-3s.

seismic weight - story 1-2	W_i	[kN]	416
seismic weight - story 3	W_{top}	[kN]	238
axial force at base columns due to gravity loads	$N^{col}_{gravity}$	[kN]	178
data derived from the step 1 (assessment)			
base shear (elastic spectrum)	V_b	[kN]	455
allowable base shear (buckling of base columns)	V^*_b	[kN]	390
reduction factor	η^*	-	0.8576
required equivalent viscous damping	ξ^{CBF}	[%]	8.6

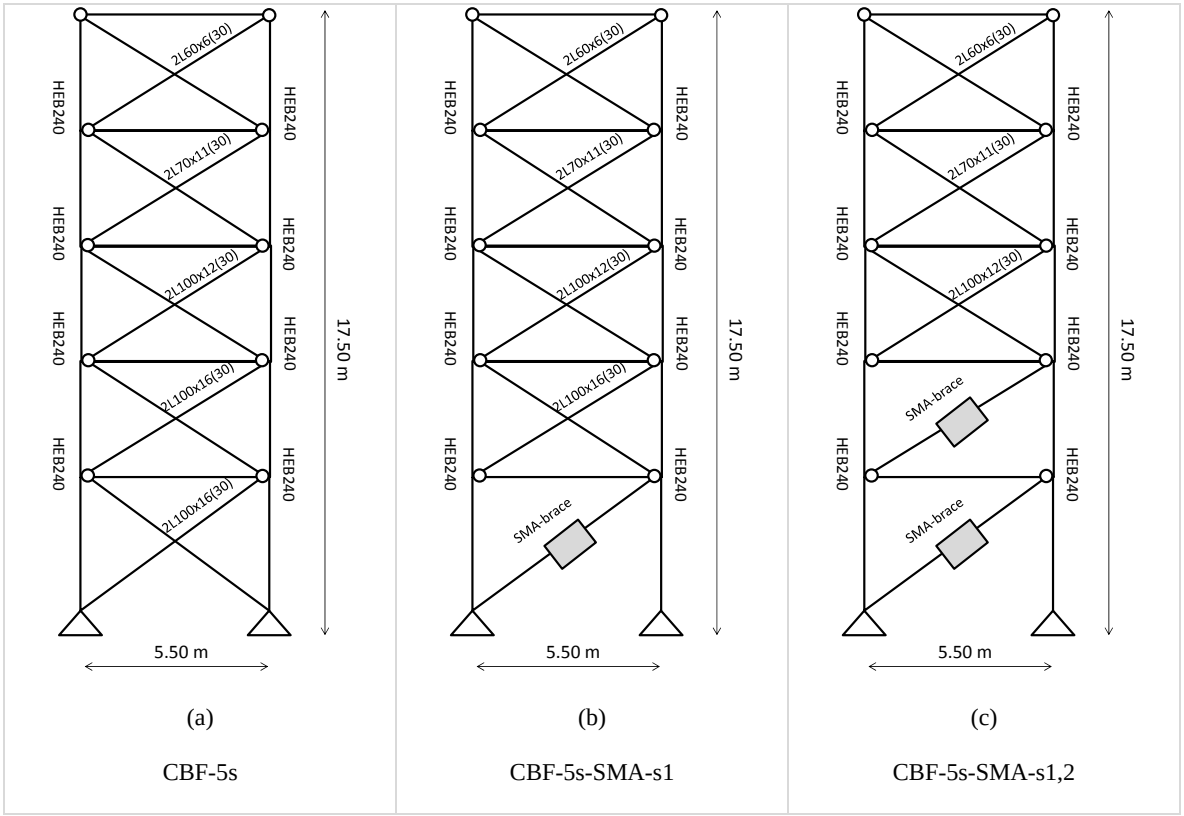

Fig. (5). Accounted five-story CBF cases: (a) un-retrofitted case; (b)-(c) retrofitted solutions.

Table 2. Parameters characterizing the un-retrofitted case of study: CBF-5s.

seismic weight - story 1-4	W_i	[kN]	416
seismic weight - story 5	W_{top}	[kN]	238
axial force at base columns due to gravity loads	$N^{col}_{gravity}$	[kN]	317
data derived from the step 1 (assessment)			
base shear (elastic spectrum)	V_b	[kN]	808
allowable base shear (buckling of base columns)	V^*_b	[kN]	697
reduction factor	η^*	-	0.86
required equivalent viscous damping	ξ^{CBF}	[%]	8.43

With reference to these case studies, the following retrofit strategies have been considered (Figs. **4b-e**, **5b**, **c**):

- *CBF-3s-SMA-s1*: three-story CBF equipped with one SMA-brace device at the first story;
- *CBF-3s-SMA-s2*: three-story CBF equipped with one SMA-brace device at the second story;
- *CBF-3s-SMA-s3*: three-story CBF equipped with one SMA-brace device at the third story;
- *CBF-3s-SMA-s1,2*: three-story CBF equipped with two SMA-brace devices respectively at first and second

story, where the secant stiffness of SMA-brace devices has been assumed proportional to the seismic story shear distribution;

− *CBF-5s-SMA-s1*: five-story CBF equipped with one SMA-brace device at the first story;

− *CBF-5s-SMA-s1,2*: five-story CBF equipped with two SMA-brace devices respectively at the first and the second story, where the secant stiffness of SMA-brace devices has been assumed proportional to the seismic story shear distribution.

3.1. Obtained Retrofitted Solutions

According to the procedure at the basis of the proposed approach, a preliminary check of the un-retrofitted CBF has been performed with the aim to identify the type of the potential ultimate mechanism, the allowable seismic force (V_b*), the required level of reduction of the seismic forces (η*) and the level of damping ratio (ξ^{CBF}) required to the retrofitted solution (Tables **1**, **2**).

For both the preliminary step of assessment and the subsequent ones, the design seismic actions have been derived according to the Italian regulations [5] by accounting for the response seismic spectrum shown in Fig. (**6**) (target spectrum) and considering the equivalent static force procedure for deriving the design base shear V_b. In particular, since the ultimate mechanism of both the accounted cases is characterized by the attainment of the buckling resistance of the columns at the base, the elastic spectrum has not been reduced through any behavior factor and, moreover, the spectral acceleration value $S_e(T)$=0.5g corresponding to the plateau of the spectrum has been considered for evaluating the design base shear V_b.

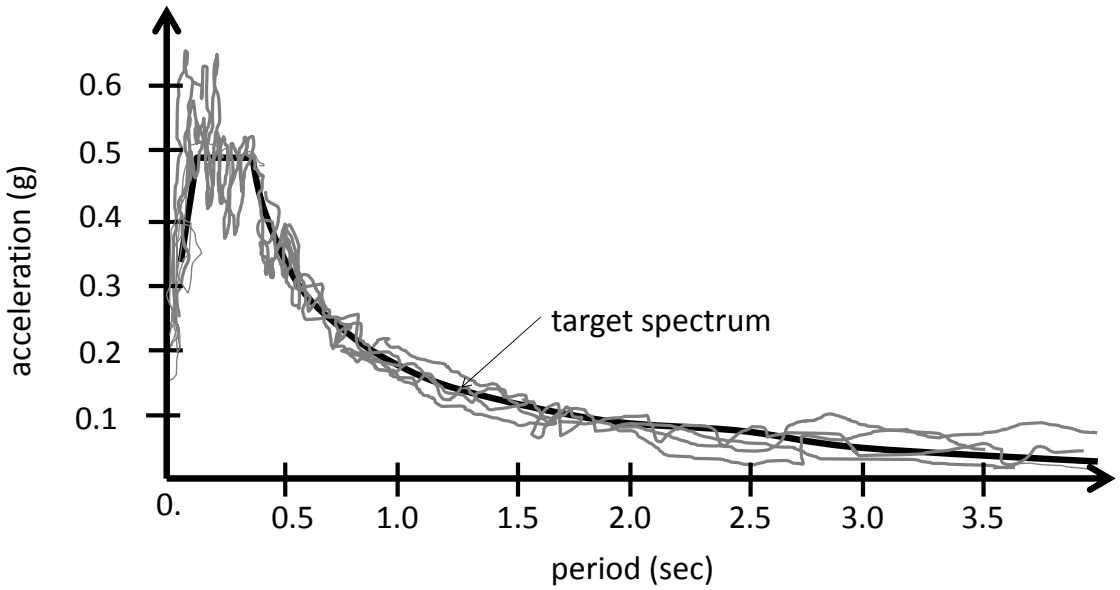

Fig. (6). Spectra of the selected accelerograms and comparison with the accounted elastic spectrum [21].

The main parameters concerning the retrofitted cases are reported in Tables **3** to **6** for the three-story case, and in Tables **7** and Table **8** for the five-story case. From the tables it is possible to observe that the parameters characterizing the SMA-brace devices are strictly influenced by the selected retrofit strategy, i.e. the number/arrangement of devices and the rule for distributing the secant stiffness at each story of the CBF.

Table 3. Parameters characterizing the CBF-3s-SMA-s1 solution.

equivalent viscous damping	ξ^{CBF}	[%]	8.6
SMA brace secant stiffness-story 1	$K^{SMA}_{sec,1}$	[N/mm]	1.0739e+005
SMA brace secant stiffness-story 1/diagonal elastic stiffness-story 1	$K^{SMA}_{sec,1}/K^{DIAG}_{el,1}$	-	0.9493
SMA brace cross section area - story 1	A^{SMA}_{1}	[mm^2]	797.39
SMA brace length - story 1	L^{SMA}_{1}	[mm]	71.78

Table 4. Parameters characterizing the CBF-3s-SMA-s2 solution.

equivalent viscous damping	ξ^{CBF}	[%]	8.6
SMA brace secant stiffness-story 2	$K^{SMA}_{sec,2}$	[N/mm]	5.5881e+004
SMA brace secant stiffness-story 2/diagonal elastic stiffness-story 2	$K^{SMA}_{sec,2}/K^{DIAG}_{el,2}$	-	0.6183
SMA brace cross section area - story 2	A^{SMA}_{2}	[mm^2]	629.15
SMA brace length - story 2	L^{SMA}_{2}	[mm]	108.84

Table 5. Parameters characterizing the CBF-3s-SMA-s3 solution.

equivalent viscous damping	ξ^{CBF}	[%]	8.6
SMA brace secant stiffness-story 3	$K^{SMA}_{sec,3}$	[N/mm]	9.0298e+003
SMA brace secant stiffness-story 3/diagonal elastic stiffness-story 3	$K^{SMA}_{sec,3}/K^{DIAG}_{el,3}$	-	0.2068
SMA brace cross section area - story 3	A^{SMA}_{3}	[mm^2]	290.91
SMA brace length - story 3	L^{SMA}_{3}	[mm]	311.43

Table 6. Parameters characterizing the CBF-3s-SMA-s1,2 solution.

equivalent viscous damping	ξ^{CBF}	[%]	8.6
SMA brace secant stiffness-story 1	$K^{SMA}_{sec,1}$	[N/mm]	6.2633e+005
SMA brace secant stiffness-story 2	$K^{SMA}_{sec,2}$	[N/mm]	4.9418e+005
SMA brace secant stiffness-story 1/diagonal elastic stiffness-story 1	$K^{SMA}_{sec,1}/K^{DIAG}_{el,1}$	-	5.5366
SMA brace secant stiffness-story 2/diagonal elastic stiffness-story 2	$K^{SMA}_{sec,2}/K^{DIAG}_{el,2}$	-	5.4682
SMA brace cross section area - story 1	A^{SMA}_{1}	[mm^2]	797.39
SMA brace cross section area - story 2	A^{SMA}_{2}	[mm^2]	629.15
SMA brace length - story 1	L^{SMA}_{1}	[mm]	12.31
SMA brace length - story 2	L^{SMA}_{2}	[mm]	12.31

Table 7. Parameters characterizing the CBF-5s-SMA-s1 solution.

equivalent viscous damping	ξ^{CBF}	[%]	8.43
SMA brace secant stiffness-story 1	$K^{SMA}_{sec,1}$	[N/mm]	8.7378e+004
SMA brace secant stiffness-story 1/diagonal elastic stiffness-story 1	$K^{SMA}_{sec,1}/K^{DIAG}_{el,1}$	-	0.4671
SMA brace cross section area - story 1	A^{SMA}_{1}	[mm^2]	1.4246e+003
SMA brace length - story 1	L^{SMA}_{1}	[mm]	157.6104

Table 8. Parameters characterizing the CBF-5s-SMA-s1,2 solution.

equivalent viscous damping	ξ^{CBF}	[%]	8.44
SMA brace secant stiffness-story 1	$K^{SMA}_{sec,1}$	[N/mm]	2.5858e+005
SMA brace secant stiffness-story 2	$K^{SMA}_{sec,2}$	[N/mm]	2.3848e+005
SMA brace secant stiffness-story 1/diagonal elastic stiffness-story 1	$K^{SMA}_{sec,1}/K^{DIAG}_{el,1}$	-	1.3823
SMA brace secant stiffness-story 2/diagonal elastic stiffness-story 2	$K^{SMA}_{sec,2}/K^{DIAG}_{el,2}$	-	1.2748
SMA brace cross section area - story 1	A^{SMA}_{1}	[mm^2]	1.4243e+003
SMA brace cross section area - story 2	A^{SMA}_{2}	[mm^2]	1.3136e+003
SMA brace length - story 1	L^{SMA}_{1}	[mm]	53.2469
SMA brace length - story 2	L^{SMA}_{2}	[mm]	53.2469

In particular, regarding the three-story case, the greatest value of the secant stiffness corresponds to the solution with two devices (in this case the devices are characterized by a secant stiffness about five times the elastic stiffness of the corresponding steel diagonals of the un-retrofitted case). On the opposite hand, the case with one device located at the third story is characterized by the lowest value of the secant stiffness (about 0.21 times of the elastic stiffness of the

corresponding steel diagonal). These differences influence the length of the deformable part of the SMA-brace device. Indeed, since the cross section area of the SMA-brace device depends on the seismic story shear (i.e. on the position along the height of the SMA-brace device) and on the ultimate strength of the SMA material (Table **9**), the greatest value of the length just corresponds to the case CBF-3s-SMA-s3.

Table 9. Parameters characterizing the SMA material [10].

Elasticity modulus austenite	E^{1}_{SMA}	[MPa]	30000
Elasticity modulus martensite	E^{2}_{SMA}	[MPa]	1628
austenite to martensite starting stress	$\sigma_{s,AS}^{SMA}$	[MPa]	510
austenite to martensite finishing stress	σ_{fAS}^{SMA}	[MPa]	580

Regarding the five-story case study, where only two retrofit strategies have been considered, similar observations can be made. Indeed, the greatest value of the secant stiffness corresponds to the case with two devices. Nevertheless, considering the three-story case, it is possible to observe significant lower values of the ratio between the elastic stiffness of the SMA-brace device and the elastic stiffness of the corresponding removed steel diagonals. This evidence underlines that, according to the structure and the hypotheses of the proposed procedure and the corresponding equations for deriving the secant stiffness of SMA-brace devices, the retrofit solution is strictly correlated to the characteristics of the case to retrofit. In fact, considering **eqn.9**, it is possible to observe that, since the level of the required damping is similar for both the three and the five story case, the greater number of steel diagonals, together with their greater elastic stiffness of the five-story case lead to a reduced value of the required secant stiffness of SMA-brace devices.

4. NON-LINEAR TIME-HISTORY ANALYSES

Once the retrofitted cases have been derived throughout the proposed approach, non-linear time-history analyses (NLTH) have been performed by using the software OPENSEES [20]. In this case, seven real accelerograms scaled in order to match the accounted elastic spectrum (Fig. **6**) have been selected through the software SEISM-HOME [21] and, according to [4], the obtained results have been averaged for assessing the capability of the proposed approach to furnish reliable solutions.

4.1. F.E. Modeling Approach

In agreement with the approach proposed in [17], the steel diagonals composing the CBF are modeled by using the inelastic beam-column brace model proposed by Uriz *et al*. [22]: each diagonal is schematized through two inelastic beam-column elements by providing a displacement for the middle joint devoted to account the initial camber of the frame, and introducing the corotational theory to account for the moderate to large deformation effects of inelastic buckling of the braces. The Giuffré–Menegotto–Pinto material model [23] with kinematics and isotropic hardening is assumed introducing a strain hardening ratio equal to 0.5%, a Young's modulus equal to 206 GPa and a yield stress of 235MPa.

Regarding the modeling of the SMA-brace devices, they are schematized through inelastic beam-column elements by introducing the uniaxial self-centering material model [24, 25]. In particular, starting from the configuration of the device consisting of a rigid segment connected to a SMA member where the deformation occurs (it is assumed that the majority of the deformation just occurs in the less stiff SMA specimen whilst the remaining portion of the brace only undergo minimal deformation and no buckling), the initial stiffness of the brace depends on the length of the SMA segment and cross-section area of SMA material: two design parameters accounted in the proposed approach. It is evident that the actual non-SMA segment may undergo some deformation in an real SMA-brace device, resulting in somewhat higher displacements. Nevertheless, for the purpose of this study, a rigid segment is assumed.

For both steel and SMA-brace devices, a fiber discretization for the cross-section of diagonals is assumed considering eight integration points and using the Newton algorithm for the iterative procedure.

Differently from the steel diagonals, a linear-elastic behavior is accounted for both the columns and beams (for beams translational constraints are also introduced in order to simulate the effect of rigid slabs). Indeed, for the un-retrofitted case the aim of NLTH analyses is to obtain the maximum ratio between the demand in terms of axial force in the columns and the corresponding strength in terms of buckling resistance. The assumed modeling strategy just allows to derive the maximum axial force demand from each NLTH analysis and, then, according to [4], to obtain the

corresponding average value.

Finally, beam-to-column connections, steel diagonals-to-column/beam connections and SMA-brace devices-to-column/beam connections are assumed as pinned without modeling gusset plates; column-to-column connections are considered as rigid in order to schematize the columns as continuous elements.

4.2. Results and Considerations

The results derived from NLTH analyses are shown in Figs. (**7** and **8**) in terms of maximum interstory drift (*i.e*. the ratio between the story relative displacement and the story height), in (Figs. **9** and **10**) in terms of maximum ratio between the axial force and the buckling resistance of the base columns of the CBF, in Fig. (**11**) in terms of required damping, and in (Figs. **12** and **13**) in terms of axial force *vs*. axial deformation of both the steel diagonals and the SMA-brace devices. In some of the graphs it is also reported the corresponding average value of the peak response for each of the accounted accelerograms.

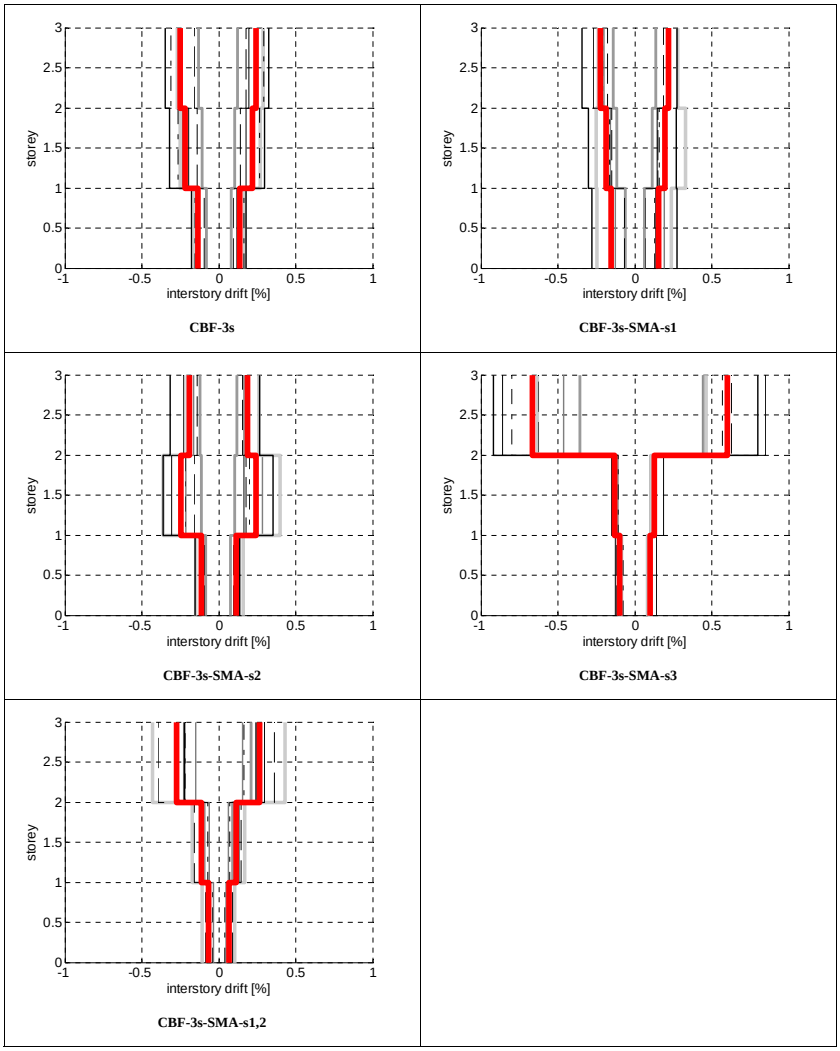

Fig. (7). Three-story CBF: maximum interstory drift values derived from NLTH analyses (thick line: average value).

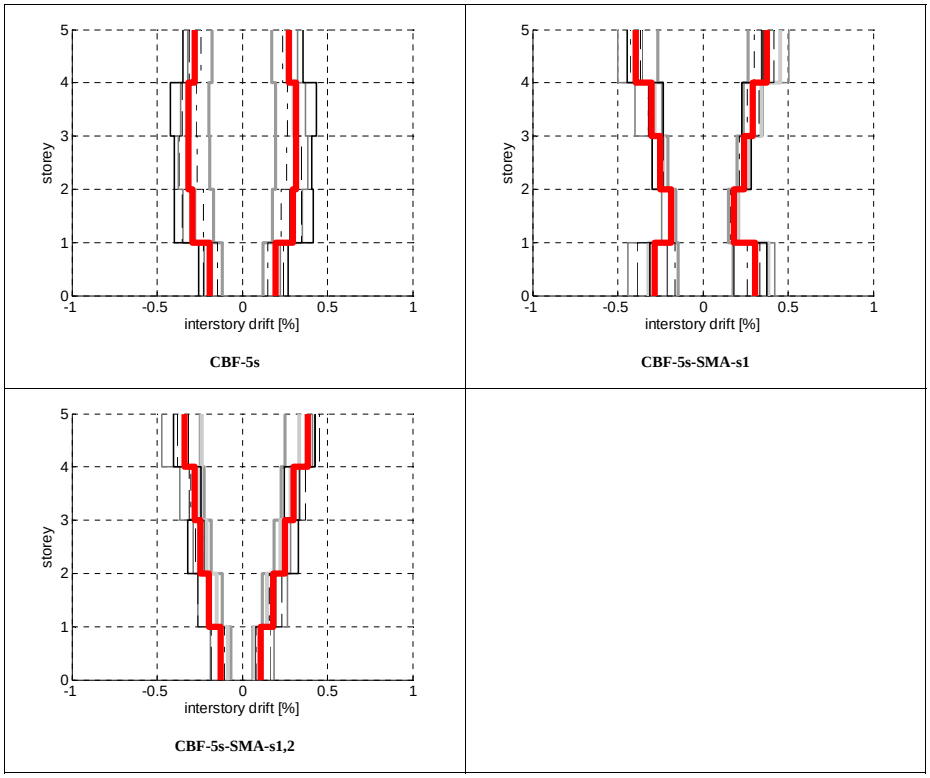

Fig. (8). Five-story CBF: maximum interstory drift values derived from NLTH analyses (thick line: average value).

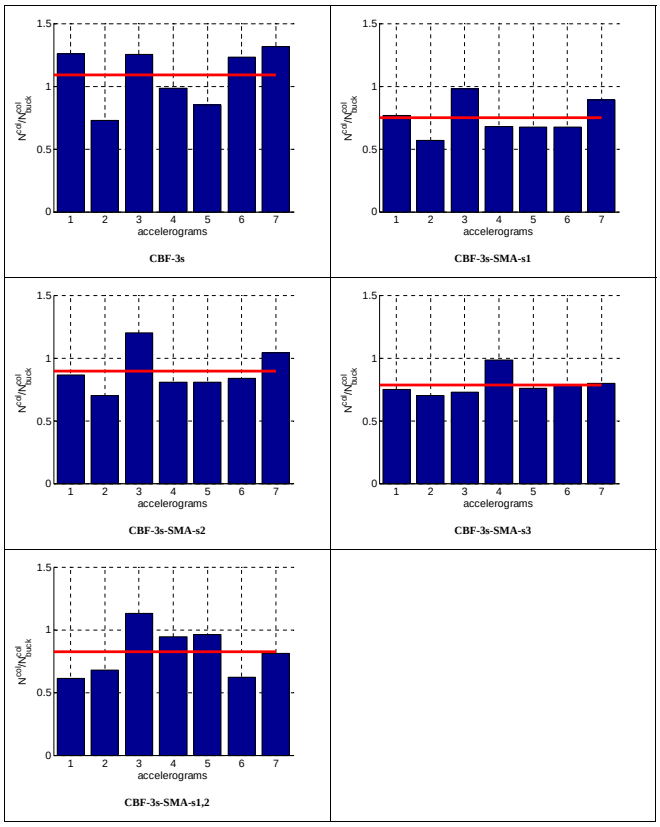

Fig. (9). Three-story CBF: maximum values of the ratio between the axial force and the buckling resistance of base columns derived from NLTH analyses (thick horizontal line: average value).

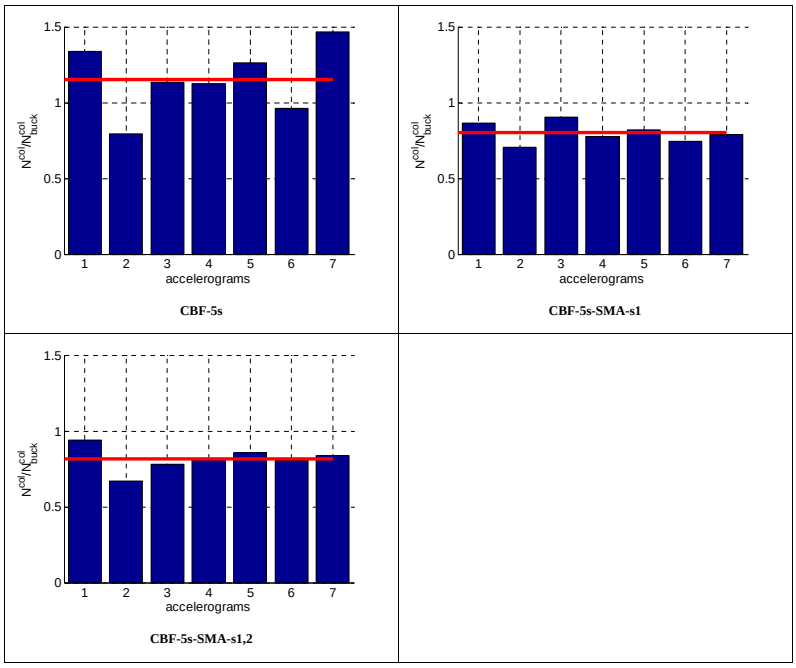

Fig. (10). Five-story CBF: maximum values of the ratio between the axial force and the buckling resistance of base columns derived from NLTH analyses (thick horizontal line: average value).

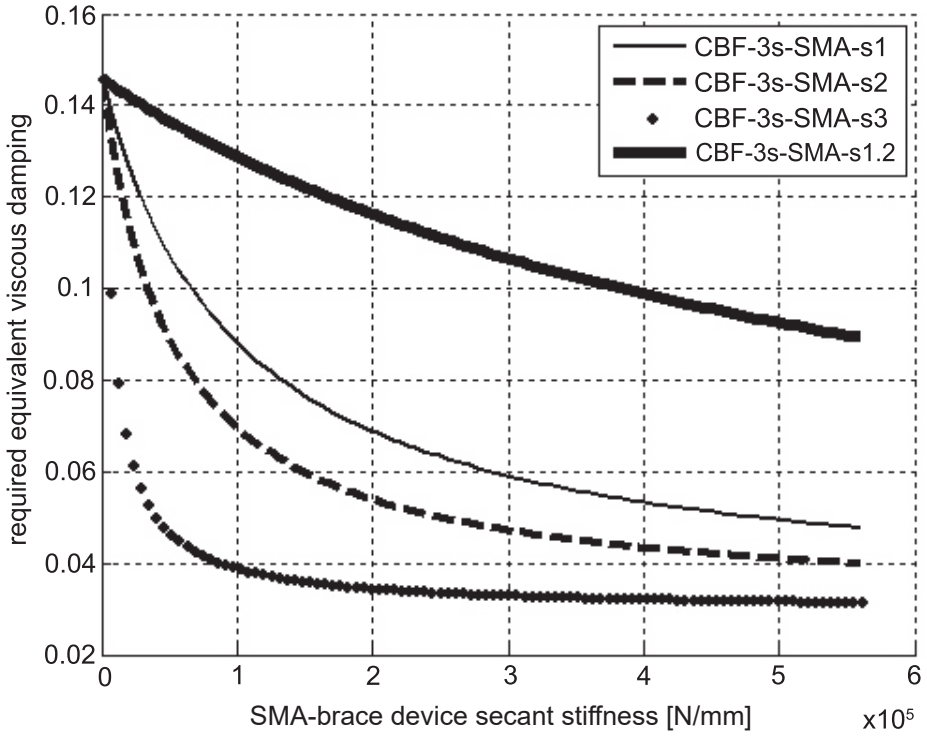

Fig. (11). Required equivalent viscous damping *vs*. SMA-brace device secant stiffness for the accounted retrofit strategies.

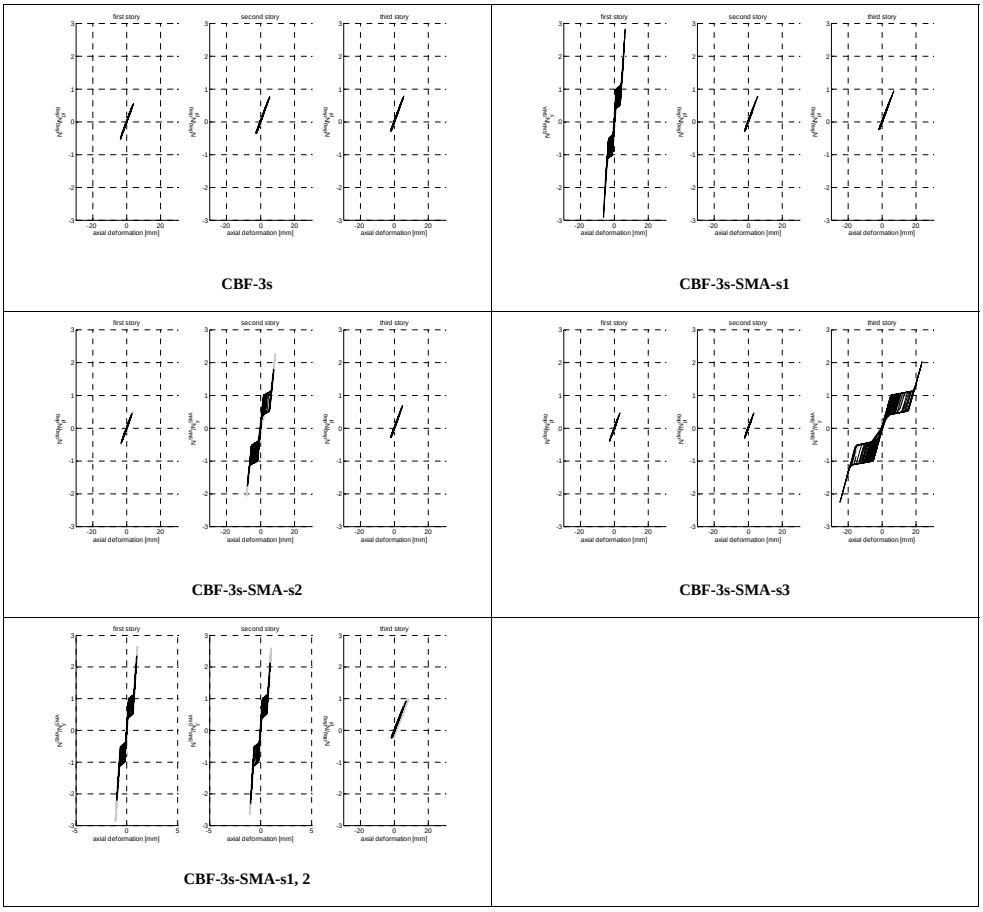

Fig. (12). Three-story CBF: axial force *vs*. axial deformation curves of steel diagonals and SMA-brace devices obtained from NLTH analyses.

Comparing the distribution along the height of the average value of interstory drifts of the un-retrofitted and the retrofitted cases (Figs. **7**, **8**), it is evident the influence of the SMA-brace devices in terms of lateral stiffness. This particularly depends on the difference between the elastic stiffness of the brace devices and the elastic stiffness of the removed steel diagonals. Indeed, while the solution CBF-3s-SMA-s1 does not show significant differences with respect to the un-retrofitted case (the elastic stiffness of the SMA-brace device located at the first story is quite similar to the elastic stiffness of the removed diagonals), the other cases show an increase or a decrease of the interstory drifts and a consequent variation of the profile of interstory drifts along the height. Nevertheless, it is also important to underline that the shape of interstory drifts it also influenced by the post-yield behavior of the SMA-brace devices.

By examining the same results it is also interesting to observe the significant increase of the interstory drifts when the SMA-brace device is located at the top story (CBF-3s-SMA-s3): this effect is due to both the significant lower secant stiffness of the SMA-brace device, but also to the position at the top story. Indeed, as observed in [2, 3] the yielding of braces at the top story leads amplification of the story drifts respect to the case of yielding of braces at intermedia stories. On the other hand, it is important to notice that the introduction of two SMA-devices with secant stiffness obtained by considering the distribution along the height of the seismic story shear, leads to a profile of interstory drifts gradually increasing along the height. This evidence is common to both the three and five-story case and it underlines that the retrofit intervention influences both the capacity of CBF to dissipate seismic forces and, at the same time, its lateral stiffness.

It is evident that the criterion for distributing the stiffness of braces along the height particularly influence the response of the retrofitted CBF and then the performance of SMA-devices. Although other solutions are possible, for instance considering the modal shapes, in this paper the distribution according to the seismic shear has been considered.

The different values of the secant stiffness of the SMA-brace devices depend on both the accounted strategy, *i.e*. the number and the arrangement of devices, and on the value of the required damping derived with reference to the un-

retrofitted solution. Indeed, in Fig. (**9**) it is graphically reported the **eqn.9** specifically for the four accounted retrofit solutions of the three-story case. This plot clearly underlines the influence of these parameters on the secant stiffness of the SMA-devices deduced through the proposed approach.

Considering the average value of the ratio between the maximum axial force at the base columns emerged during the NLTH analyses and the corresponding buckling resistance (Figs. **9**, **10**), it emerges that, while for the un-retrofitted cases values of axial forces greater than the admissible ones emerge, all the retrofitted solutions show values of the average ratio lower than the admissible one. In fact, while for the unretrofitted cases the majority of the seven accounted accelerograms leads to maximum axial forces at the base columns significantly greater than the buckling resistance, in the case of the retrofit solutions this evidence only emerges for the cases CBF-SMA-s2 and CBF-SMA-s1,2 for few accelerograms (two accelerograms for the case CBF-SMA-s2 and one accelerogram for the case of CBF-SMA-s1,2). Also in the case of the five-story CBF, for both the accounted retrofit solutions result axial forces lower than the buckling resistance. These evidences confirm the ability of the proposed design approach to opportunely improve the seismic behavior of CBFs by increasing their ability to dissipate the input seismic energy thanks to the presence and the effectiveness of the SMA-brace devices, which then results correctly designed.

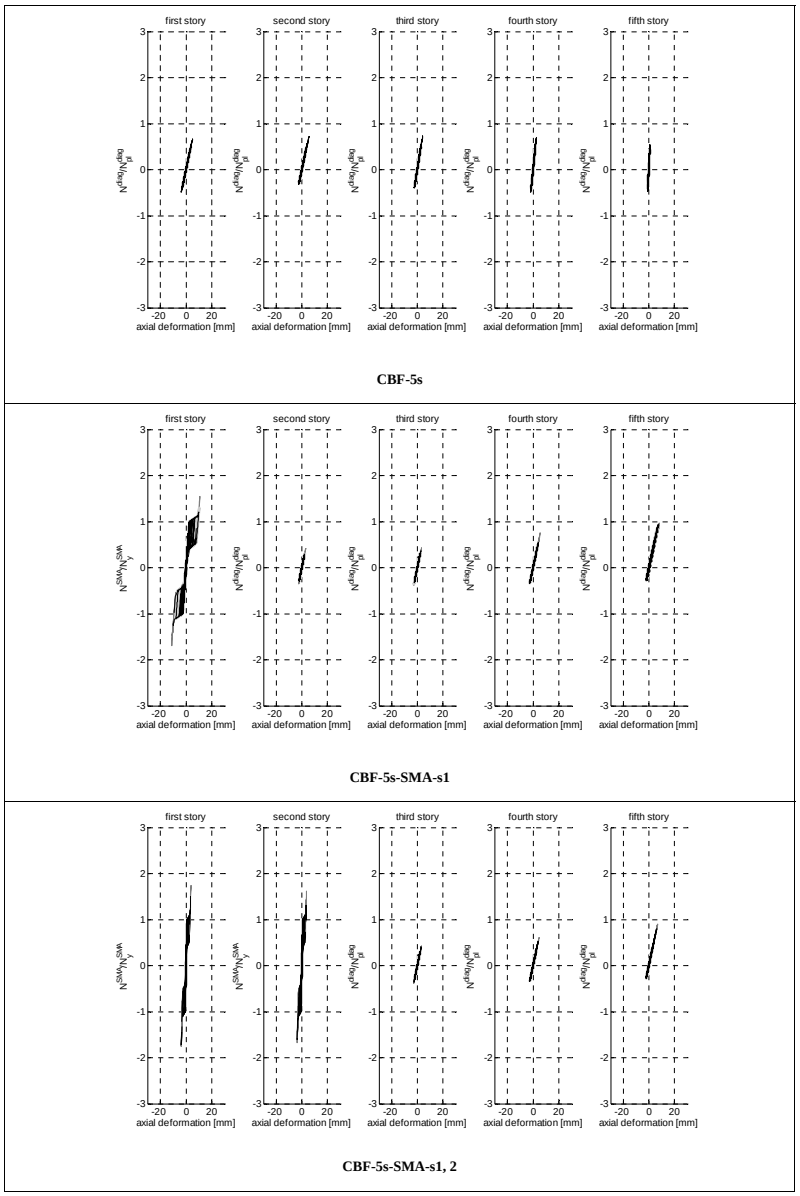

Fig. (13). Five-story CBF: axial force *vs*. axial deformation curves of steel diagonals and SMA-brace devices obtained from NLTH analyses.

Finally, examining the graphs reporting axial force *vs*. axial deformation of both SMA-devices and steel diagonals (Figs. **12**, **13**) it is possible to observe that:

- Although the presence of SMA-brace devices leads to a variation of the lateral stiffness of CBFs, all the retrofit solutions are characterized by axial force values in the steel diagonals lower than the yield strength. This evidence is in agreement with the aim of the proposed design procedure where the damping to provide to the CBF is just evaluated by considering an elastic behavior of steel diagonals. Indeed, since the proposed approach is a force-based method, the evaluated damping directly comes from considerations on the design forces and the allowable forces in the members, i.e the ones corresponding either to the buckling of columns/beams or to the yielding of slenderness diagonals.
- It is important to observe that, the cases accounted in the paper are both characterized by an allowable seismic base shear corresponding to the buckling of the base columns, which precedes the attainment of the yield strength of steel diagonals. Consequently, since the aim of the retrofit is to reduce axial forces in the columns by increasing the energy dissipation capacity of CBFs, axial forces in the steel diagonals lower than their yield strength characterize the obtained retrofitted cases.
- A further important aspect, strictly dependent on the efficacy of the proposed approach, is that the SMA-brace devices exhibit a wide post-yield behavior by attaining for the majority of the accounted accelerograms the axial displacement corresponding to the end of the Austenite-Martensite transformation phase. This represents another important evidence since, in agreement with the aim of the proposed approach, it allows to dissipate the maximum amount of input energy through the SMA-brace devices (a further criterion at the basis of the proposed design procedure).

CONCLUSION

Retrofit interventions are often performed by introducing in structures dissipative devices able to improve the global seismic response particularly in terms of energy dissipation capacity. In the case of CBFs, these devices are generally introduced as brace elements made of different materials and based on different dissipation mechanisms. The design of the retrofit intervention is strictly related to both the characteristics of the selected device and, also, to the own peculiarities of the structural system object of the retrofit intervention.

The paper has presented a simple design approach concerning SMA-brace devices for the seismic retrofit of CBFs. The procedure at the basis of the proposed approach considers both the characteristics of SMA materials and, at the same time, the main peculiarities of the seismic response of CBF structural systems. Indeed, the whole procedure is based on simple equilibrium considerations just taking into account the truss resistant mechanism of CBFs. They allow to derive axial forces in the members and, then, to obtain information regarding the seismic capacity of CBFs (in terms of allowable seismic shear) and the corresponding potential ultimate mechanism. The first phase of the proposed approach is just finalized to derive these information in order to assess the need to retrofit interventions and the required damping level. Indeed, since the proposed approach considers a force-based method, the required damping is evaluated on the basis of the design value of seismic shear and the derived allowable value, the latter strictly correlated to the ultimate mechanism.

The use of SMA-brace devices for retrofit interventions has particularly influenced the equations at the basis of the proposed approach. In particular, the assumption of guaranteeing the maximum damping level of SMA influences the characteristics of the SMA-devices in terms of secant stiffness. On the other hand, since the SMA-brace devices are inserted in lieu to steel diagonals, the amount in terms of SMA materials (cross-section area) is strictly dependent on the sustained seismic force. This could particularly influence the cost of the retrofit intervention, the arrangement of SMA-devices and the level of damping to furnish to CBFs. A further important parameter derived at the end of the approach is the length of the SMA wires/bars: this represents an important information for the practical design of the device.

The numerical analyses developed with reference to three and five-story CBFs considering different retrofit strategies, have underlined the reliability of the proposed approach. Indeed, in addition to the predicted level of reduction of strength requirements to the columns of the CBF, the proposed approach is able to preserve the steel diagonals from the yielding and to guarantee the attainment of stress levels of the SMA material corresponding to the end of the Austenite-Martensite transformation phase: these are two important criteria at the basis of the proposed approach for the retrofit of CBFs through SMA-brace devices.

The results derived from NLTH analyses have also emphasized the influence of SMA-brace devices on the profile of interstory drifts, which particularly depends on both the accounted retrofit strategy (number and arrangement of SMA-brace devices) and the characteristics of the accounted un-retrofitted case. This evidence underlines that the retrofit intervention obtained from the proposed approach leads to a variation of the seismic response of CBFs not only in terms of energy dissipation capacity, but also in terms of lateral stiffness: two key parameters in a retrofit intervention.

A further observation concerns the assumption of a fixed triangular shape of lateral seismic forces for evaluating axial forces in members (according to the accounted guidelines): this makes the proposed approach particularly devoted to buildings where the dynamic response is not significantly influenced by higher modes of vibration. This aspect has to be considered when the obtained solution is based on the introduction of SMA-brace devices which could modify the lateral stiffness of CBFs leading to an irregular seismic behavior along the height [3].

Finally, it is important to underline that the proposed approach can be applied also in case of ultimate mechanisms involving the yielding of one or more steel diagonals: the structure of the proposed procedure remains the same. Indeed, since the elastic design of CBFs generally allows to use diagonals with high slenderness ratios, these elements are not able to guarantee adequate levels of energy dissipation. Consequently, in this case the role of SMA-brace devices is to avoid yielding phenomena in these members.

The proposed approach has been developed by considering a common configuration of SMA-devices characterized by a rigid part and a deformable portion composed of SMA wires or bars. Indeed, since the cost of SMA is one of the disadvantages to using these materials, the proposed approach allows to optimize the amount of SMA material in terms of cross-section area and length of wires/bars: two design parameters specifically considered as input/output data. This allows to compare the different solutions in terms of both structural performance and in terms of costs.

LIST OF SYMBOLS

$\xi_{hyst,max,i}^{SMA}$ = Maximum Equivalent Viscous Damping Ratio Provided by the SMA-Brace Devices

$\sigma_{f,AS}^{SMA}$ = Stress of the SMA Material at the end of the Austenite-Martensite Transformation Phase

V^*_b = Allowable Seismic base Shear of CBF

V_b = Seismic Design Base Shear Derived from National Guidelines

η^* = Required Level of Reduction of the Seismic Forces

ξ^{CBF} = Equivalent Viscous Damping Ratio Required for Retrofitting the CBF

ξ_I^{CBF} = Initial Damping Coefficient into Elastic Range

ξ_{hyst}^{CBF} = Hysteretic Damping Coefficient due to the Non-Linear Behavior of CBF

E_D^{CBF} = Dissipated Energy of the CBF

E_{s0}^{CBF} = Stored Energy of the CBF

$E_{D,i}^{SMA}$ = Energy Dissipated by the SMA-Brace Device at the Story *i*

$N_{u,i}^{SMA}$ = Axial Force of the SMA-Brace Device at the Story I Corresponding to the Attainment of the Maximum Equivalent Viscous Damping Level of SMA

$\Delta L_{u,i}^{SMA}$ = Axial Deformation of the SMA-Brace Device at the Story i Corresponding to the Attainment of the Maximum Equivalent Viscous Damping Level of SMA

$K_{sec,i}^{SMA}$ = Secant Stiffness of the SMA Brace Device at the Story *i*

$K_{el,i}^{diag}$ = Elastic Stiffness of the Steel Diagonal at the Story *i*

$\gamma_{V,i}$ = Ratio Between the Shear $V_{b,i}$* at the Story *i* of the CBF and the Base Shear V_b*

E_{steel} = Young's Modulus of the Steel Material Composing the Diagonal

A_i^{diag} = Cross Section Area of the Steel Diagonal at the Story *i*

L_i^{diag} = Length of the Steel Diagonal at the Story *i*

θ_i = Angle of Inclination of the Steel Diagonal at the Story *i* to the Horizontal

A_i^{SMA} = Cross Section Area of the SMA-Brace Device at the Story *i*

$N_{y,i}^{SMA}$ = Yielding Axial Resistance of the SMA-Brace Device at the Story *i*

$N_{u,i}^{SMA}$ = Ultimate Axial Resistance of the SMA-Brace Device at the Story *i*

$K_{1,i}^{SMA}$ = Elastic Stiffness of the SMA-Brace Device at the Story *i* in the Austenite Phase

L_i^{SMA} = Length of the Deformable Portion of the SMA-Brace Device at the Story *i*

CONSENT FOR PUBLICATION

Not applicable.

CONFLICT OF INTEREST

The authors declare no conflict of interest, financial or otherwise.

ACKNOWLEDGEMENTS

Declared none.

REFERENCES

[1] G. Brandonisio, M. Toreno, E. Grande, E. Mele, and A. De Luca, "Seismic design of X concentric braced frames", *J. Construct. Steel Res.,* vol. 78, pp. 22-37, 2012.
[http://dx.doi.org/10.1016/j.jcsr.2012.06.003]

[2] E. Grande, and A. Rasulo, "Seismic assessment of concentric X-braced steel frames", *Eng. Struct.,* vol. 49, pp. 983-995, 2013.
[http://dx.doi.org/10.1016/j.engstruct.2013.01.002]

[3] E. Grande, and A. Rasulo, "Seismic assessment and retrofit of steel CBF", *Proceedings of 7th European Conference on Steel and Composite Structures (EUROSTEEL 2014),* pp. 639-630, 2014.

[4] European Committee for Standardization — Eurocode 8. Design of structures for earthquake resistance. Part 1: General rules. EN1998-1-2004. CEN., Seismic Actions and Rules for Buildings: Brussels, 2004..

[5] Ministero dei Lavori Pubblici — Norme Tecniche per le Costruzioni, *Decreto Ministeriale 14 gennaio,* .

[6] T.T. Soong, and G.F. Dargush, *Passive Energy Dissipation Systems in Structural Engineering,* Wiley & Sons, 1997.

[7] M. D'Aniello, G. Della Corte, and F.M. Mazzolani, "Experimental tests of a real building seismically retrofitted by special buckling restrained braces", *AIP Conference Proceedings,* pp. 1513-1520, 2008.
[http://dx.doi.org/10.1063/1.2963777]

[8] A.S. Pall, and C. Marsh, "Response of friction damped braced frames", *J. Struct. Eng.,* vol. 108, no. 9, pp. 1313-1323, 1982.

[9] R. Sabelli, S. Mahin, and C. Chang, "Seismic demands on steel braced frame buildings with buckling-restrained braces", *Eng. Struct.,* vol. 25, no. 5, pp. 655-666, 2003.
[http://dx.doi.org/10.1016/S0141-0296(02)00175-X]

[10] D. Fugazza, *"Use of Shape-Memory Alloy Devices in Earthquake Engineering: Mechanical Properties Advanced Constitutive Modelling and Structural Applications"*, PhD Thesis*,* Università degli Studi di Pavia - ROSE School European School for Advanced Studies in Reduction of Seismic Risk, Italy, 2005.

[11] J. McCormick, R. DesRoches, D. Fugazza, and F. Auricchio, "Seismic assessment of concentrically braced steel frames with shape memory alloy braces", *J. Struct. Eng.,* vol. 133, pp. 862-870, 2007.
[http://dx.doi.org/10.1061/(ASCE)0733-9445(2007)133:6(862)]

[12] S. Bruno, and C. Valente, "Comparative response analysis of conventional and innovative seismic protection strategies", *Earthquake Eng. Struct. Dynam.,* vol. 31, pp. 1067-1092, 2002.
[http://dx.doi.org/10.1002/eqe.138]

[13] M. Dolce, D. Cardone, and R. Marnetto, "Implementation and testing of passive control devices based on shape memory alloys", *Earthquake Eng. Struct. Dynam.,* vol. 29, pp. 945-968, 2000.
[http://dx.doi.org/10.1002/1096-9845(200007)29:7<945::AID-EQE958>3.0.CO;2-#]

[14] R. Desroches, and B. Smith, "Shape memory alloys in seismic resistant design and retrofit: a critical review of their potential and limitations", *J. Earthq. Eng.,* vol. 7, no. 3, pp. 1-15, 2003.

[15] H. Ghaffarzadeh, and A. Mansouri, "Investigation of the behavior factor in SMA braced frames", *The 14th World Conference on Earthquake Engineering,* October 12-17, 2008, Beijing, China

[16] F. Auricchio, S. Marfia, and E. Sacco, "Modelling of SMA materials: Training and two way memory effects", *Comput. Struc.,* vol. 81, pp. 2301-2317, 2003.
[http://dx.doi.org/10.1016/S0045-7949(03)00319-5]

[17] E. Grande, and A. Rasulo, "A simple approach for seismic retrofit of low-rise concentric X-braced steel frames", *JCSR,* vol. 107, pp. 162-172, 2015.

[18] J.J. Bommer, A.S. Elnashai, and A.G. Weir, "Compatible acceleration and displacement spectra for seismic design codes", *Proceedings of the 12th World Conference on Earthquake Engineering*, Auckland, 2000, p. 207.

[19] L.S. Jacobsen, "Damping in composite structures", *Proceedings of 2nd world conference on earthquake engineering Tokyo and Kyoto*, Japan, 1970, pp. 1029-1044.

[20] *OpenSees — Open system for earthquake engineering simulation. Pacific Earthquake Engineering Research Center.,* University of California: Berkeley, 2006.

[21] M. Rota, E. Zuccolo, L. Taverna, M. Corigliano, C.G. Lai, and A. Penna, "Mesozonation of the Italian territory for the definition of real spectrum-compatible accelerograms", *Bull. Earthquake Eng.,* vol. 10, no. 5, pp. 1357-1375, 2012.
[http://dx.doi.org/10.1007/s10518-012-9369-4]

[22] P. Uriz, F.C. Filippou, and S.A. Mahin, "Model for cyclic inelastic buckling for steel member", *J. Struct. Eng.,* vol. 134, no. 4, pp. 619-628, 2008.
[http://dx.doi.org/10.1061/(ASCE)0733-9445(2008)134:4(619)]

[23] CEB, *RC elements under cyclic loading- state of the art report.,* Thomas Telford: London, 1996.

[24] C. Christopoulos, R. Tremblay, H.J. Kim, and M. Lacerte, "Self-centering energy dissipative bracing system for the seismic resistance of structures: Development and validation", *J. Struct. Eng.,* vol. 134, no. 1, pp. 96-107, 2008.
[http://dx.doi.org/10.1061/(ASCE)0733-9445(2008)134:1(96)]

[25] R. Tremblay, M. Lacerte, and C. Christopoulos, "Seismic response of multistory buildings with self-centering energy dissipative steel braces", *J. Struct. Eng.,* vol. 134, no. 1, pp. 108-120, 2008.
[http://dx.doi.org/10.1061/(ASCE)0733-9445(2008)134:1(108)]